Published in final edited form as:
Biochemistry. 2009 November 17; 48(45): 10716–10723. doi:10.1021/bi901205w.

Substrate Redox Potential Controls Superoxide Production Kinetics in the Cytochrome *bc* Complex†

Jonathan L. Cape‡, **Divesh Aidasani**‡, **David M. Kramer**‡, and **Michael K. Bowman**§,*

‡ Institute of Biological Chemistry, Washington State University, 289 Clark Hall, Pullman, Washington 99164-6314

§ Department of Chemistry, Box 870336, The University of Alabama, Tuscaloosa, Alabama 35487-0336

Abstract

The Q-cycle mechanism of the cytochrome bc_1 complex maximizes energy conversion during electron transport from ubiquinol to cytochrome *c* (or alternate physiological acceptors). Yet important steps in the Q-cycle are still hotly debated including: bifurcated electron transport; the high yield and specificity of the Q-cycle despite possible short circuits and bypass reactions; and the rarity of observable intermediates in the oxidation of quinol. Mounting evidence shows that some bypass reactions producing superoxide during oxidation of quinol at the Q_o site diverge from the Q-cycle rather late in the bifurcated reaction and provide an additional means of studying initial reactions of the Q-cycle. Bypass reactions offer more scope for controlling and manipulating reaction conditions, *e.g.*, redox potential, because they effectively isolate or decouple the Q-cycle initial reactions from later steps, avoiding many complications and interactions. We examine the dependence of oxidation rate on substrate redox potential in the yeast cytochrome bc_1 complex and find that the rate limitation occurs at the level of direct one-electron oxidation of quinol to semiquinone by the Rieske protein. Oxidation of semiquinone and reduction of cyt *b* or O_2 are subsequent, distinct steps. These experimental results are incompatible with models in which electron transfer to the Rieske protein is not a distinct step preceding electron transfer to cytochrome *b*, and with conformational gating models that produce superoxide by different rate limiting reactions from the normal Q-cycle.

The cytochrome (cyt[1]) bc_1 (also known as Complex III or ubiquinol:cyt c oxidoreductase) and related complexes are essential energy transduction components in the respiratory and photosynthetic electron transport chains of a wide range of organisms (1–4). Its physiological role is to pump protons across the inner mitochondrial membrane to drive synthesis of ATP, but its detailed enzyme mechanism and possible roles in oxidative stress are still disputed. Our focus is on the mitochondrial cyt bc_1 complex from *Saccharomyces cerevisiae* whose dimeric functional core is illustrated in cartoon form in the left hand side of Fig. 1. Each monomer consists of three essential catalytic subunits (2,5–8): cyt *b*; the Rieske iron-sulfur protein (ISP); and cyt c_1. The redox-active cofactors form two distinct redox chains leading away from the

†This work was supported by a grant from the National Institutes of Health GM061904.

*Phone: +1-205-348-7846; FAX: +1-205-348-9104; mkbowman@as.ua.edu.

Supporting Information Available

The syntheses of the substrate analogs used in this study and the details of the estimation of redox potentials are described in detail as Supporting Information. This material is available free of charge via the Internet at http://pubs.acs.org.

[1]Abbreviations: cyt, cytochrome; ISP, iron sulfur protein; Q_o site, quinol oxidase site; Q_i site, quinone reductase site; FeS, two iron-two sulfur cluster in the ISP; SQ, semiquinone; SQ_o, semiquinone in Q_o; *pmf*, Proton motive force; AA, Antimycin A; MOA, methoxyacrylate; EPR, electron paramagnetic resonance; NMR, nuclear magnetic resonance; ESI, electrospray ionization; SOD, superoxide dismutase; K_m, Michaelis constant; V_{max}, maximum rate of reaction; K_i, inhibition constant.

quinol oxidase (Q_o) site on the positive side (*p*-side) of the membrane (5). A 'low-potential chain' extends across the membrane from the Q_o site, through the cyt *b* subunit with its two *b*-type hemes (cyt b_L and cyt b_H), to the quinone reductase (Q_i) site on the negatively-charged side (*n*-side) of the membrane. The 'high-potential chain' consists of the Rieske FeS cluster of the ISP, and the *c*-type heme of cyt c_1. This chain, on the *p*-side of the membrane, relays electrons from the Q_o site to a soluble cyt *c*.

The cyt bc_1 complex catalyzes a Q-cycle, illustrated in Fig. 1 Left, as first proposed by Mitchell and modified extensively (9–12) as a result of the work of many researchers. In most models of the Q-cycle (1,13), QH_2—originating from complex II in *S. cerevisiae*—binds in the Q_o site and is oxidized in the so-called 'bifurcated' reaction, releasing two protons on the positively charged, *p*-side, of the membrane. The first QH_2 electron enters the high-potential chain at the Rieske FeS cluster. A pivoting motion of the Rieske ISP (shown as two superimposed conformations in Fig. 1 Left) carries its FeS cluster close to cyt c_1, allowing reduction of the cyt c_1, which then relays the electron to a soluble cyt *c*. Eventually the electrons arrive at complex IV where they reduce O_2 to water.

In this model of the Q-cycle, the one-electron oxidation of QH_2 at Q_o forms a transient semiquinone (SQ) intermediate, termed SQ_o (14,15). Instead of reducing the thermodynamically-favored high-potential chain a second time, SQ_o reduces cyt b_L in the low-potential chain. Electrons sent into the low-potential chain travel through cyt b_H and cyt b_L, and eventually reduce a Q bound at the Q_i site. After two turnovers of the Q_o site, two electrons pass through the low potential chain, reducing Q to QH_2 at the Q_i site, with uptake of two protons from the *n*-side of the membrane. Overall, the Q-cycle oxidizes two QH_2 at Q_o, with the release of four H^+ on the *p*-side; and reduces one Q at Q_i with uptake of two H^+ from the *n*-side. The net result is a highly efficient proton pump that helps produce the transmembrane proton motive force (*pmf*) that drives ATP synthase. This complicated Q-cycle gives a stoichiometry of 2 H^+ translocated across the membrane per e^- passed ultimately to cyt *c* in the steady state, increasing the ATP synthesized per O_2 reduced (the P/O ratio) over that of a linear electron flow mechanism in which both QH_2 electrons enter the high-potential chain (16,17).

It is argued that the bifurcated electron flow also serves to 'quench' the SQ_o (18–27) and prevent its reaction with O_2 to generate superoxide. Superoxide production by the Q_o site (and other reactions that 'bypass' the Q-cycle) is readily observed by blocking the low-potential chain in a number of ways, including: high *pmf* (28–30); high membrane potential (30); mutation of cyt *b* (17,31); inhibition of the Q_i site, *e.g.* by antimycin A ('AA' in Fig 1 Right); or inhibition of the Q_o site niche near heme b_L (proximal niche), *e.g.* by myxothiazole or methoxyacrylate (MOA) stilbene ('X' in Fig. 1 Right) (21,22). Superoxide production at the Q_o site is hotly debated as a mitochondrial source of superoxide and other reactive oxygen species in processes such as cell signaling, aging, carcinogenesis and metabolic diseases.

A number of reactions 'bypass' the normal Q-cycle, reducing the efficiency of proton pumping and diverting electron flow, at least temporarily (20). The different bypass reactions are not mutually exclusive and might occur in combinations depending on conditions. We focus in this paper on the bypass reaction that produces superoxide during oxidation of quinol at the Q_o site because of its very intimate relation to the initial steps in the Q-cycle. Recently, superoxide production has recently been described through a very different bypass reaction that involves reduction of quinone at the Q_o site (32,33), but it will not be considered here.

Forquer *et al.* (34) recently showed that the rate limiting step for superoxide production in AA-inhibited mitochondrial cyt bc_1 complex is the same as for the Q-cycle—involving reduction of the Rieske FeS cluster. Thus, the Q-cycle and superoxide production share intermediates

along the same, or similar, reaction pathway(s). EPR of freeze-quenched bacterial cyt bc_1 complex suggests that this common intermediate is SQ_o (14,15). These recent results allow earlier conclusions about the order of reactions in the Q-cycle the bacterial *Rhodobacter sphaeroides* cyt bc_1 complex (35) to be extended to the mitochondrial cyt bc_1 complex.

Little superoxide is generated by cyt bc_1 under normal physiological conditions. Several classes of models attempt to explain how the Q_o site steers the reaction along the Q-cycle and away from superoxide production (14,15,34,35). The experimental evidence is increasingly at odds with models in which the oxidation of QH_2 to SQ is radically different for superoxide production than for the Q-cycle, particularly the 'double concerted' electron transfer mechanisms (13,25,27,36). Models that invoke conformational gating (6,37–41) of the Q_o site to steer electron flow are severely constrained because the same activating reaction occurs during quinol oxidation both when the putative gate functions 'normally' and when it leaks, to produce superoxide (34).

The Q-cycle and the bypass reaction pathways must diverge at some point. On this point conflicting results have been obtained depending on reaction conditions. In contrast to Forquer *et al*. (34), Covian and Trumpower (42) concluded that there are different rate limiting steps for the Q-cycle and the bypass reactions from different activation energies under pre-steady state, non-substrate-saturated conditions. The relevance of these results to the reactions of the cyt bc_1 complex is limited until the new rate limiting steps are identified and until it is determined which bypass reactions occur under these conditions. Consequently, we will restrict our discussion to substrate-saturated steady-state conditions unless explicitly stated.

Important questions still remain concerning the sequence of reactions and the redox partner of the ISP in the rate limiting step. Does quinol transfer an electron directly to the FeS cluster thereby generating SQ_o or is there an intervening step? What factors control the rate of superoxide production with other quinols as substrate? Do interactions of the enzyme with particular sidegroups of the substrate guide the reaction and determine the products? To resolve these questions we examine superoxide production in the yeast mitochondrial cyt bc_1 complex with a series of seven ubiquinol analogs designed to vary redox potentials and sidegroups on the quinol ring. One of the challenges to such work has been the limited ability to make consistent redox measurements on quinone species with the long, hydrophobic tails needed for activity. The ability to calculate these properties (43) now makes such a study feasible. We report here on the substrate properties that control the substrate saturated rate of superoxide production; we identify the rate limiting reaction; and we determine the sequence of the bifurcated electron transfer reactions.

Experimental Procedures

Chemical Syntheses

Starting materials were purchased from Sigma-Aldrich, USA and used without further purification, except as indicated. Substrates were purified by silica gel chromatography (0.035–0.07 mm particle size, 6 nm pore size, Acros, Geel, Belgium). Syntheses for most of these compounds, or close derivatives, have been described (44–47). Full details are provided as Supporting Information. Product identity was confirmed using ^1H and ^{13}C NMR spectra recorded at the Washington State University Center for NMR Spectroscopy on a Varian Mercury 300 MHz NMR spectrometer. Mass spectra were recorded on a Finnegan LCQ mass spectrometer using an ESI ionization source in negative ion mode.

Purification of the cyt bc_1 complex

Cyt bc_1 complex from *S. cerevisiae* was isolated from store-bought bakers' yeast using the protocol of Ljungdahl *et al.* (48) with modifications (22). The concentration of the cyt bc_1 complex was determined by ferricyanide-ascorbate-dithionite absorbance difference spectra using published values of the extinction coefficients (48).

Steady-State Enzyme Turnover Measurements

Steady-state turnover rates were measured from the initial rate of cyt *c* reduction (19,22). The stigmatellin-sensitive portion of the rate is reported, so that the activity can be attributed to the Q_o site. Q-cycle bypass is measured in the presence of 10 μM of the Q_i site inhibitor, AA; and the bypass rate is half the rate of cyt *c* reduction because each bypass turnover eventually transfers two electrons to cyt *c*. The rate of superoxide production was measured from the SOD-sensitive fraction of the bypass rate, recognizing that the SOD-dependent decrease in cyt *c* reduction equals the superoxide production. The initial rates follow Michaelis-Menton kinetics. The reported V_{max} are based on measurements at substrate concentrations several times larger than the measured K_m, Table 1.

The AA-inhibited complex is a reproducible model of other elicitors of superoxide production, such as mutation of certain Q_o and Q_i site residues (17,31,49,50), high *pmf* (28,30) or high membrane potential (30), in which electron transfer through the low-potential chain is slowed. The use of AA also prevents reactions of substrate at the Q_i site from influencing the measurements (see below) and eliminates the sample variability and instability noted with the use of lipid vesicles to control *pmf* or membrane potential (30). Yeast submitochondrial particles (data not shown), yielded similar results, ruling out artifacts from detergent solubilization or delipidization of the cyt bc_1 complex. Use of purified complex precludes interference from other enzymes found in crude preparations or from endogenous substrates. Forquer, *et al*. (34) found that purified complexes also avoided the kinetic artifacts (*e.g.*, nonlinear or curved responses) seen in native membranes (35) where QH_2 concentrations were near K_m.

The fast initial rates of some bypass reactions were verified by stopped-flow techniques, measuring the rate of cyt *c* reduction, as described above (see Table 1). The substrate concentrations used in stopped flow experiments were well in excess of the steady state K_m values, resulting in rates that were independent of substrate concentration. Competition assays between non-native Q-species and the native substrate analog **(3)** were used to estimate the K_i of the non-native Q species and were analyzed using a mixed competitive inhibition model (51) with simultaneous fitting of substrate titration curves over a range of quinone concentrations, holding the uninhibited K_m and V_{max} values constant. Shifts in the Q/QH_2 potential from differential Q/QH_2 binding were estimated from the ratio of competitive K_i/K_m values. In some cases decyl-ubiquinol was used in place of **(3)** (differing by one carbon in the tail) with identical results.

Thermodynamic properties of QH_2 substrates

The estimation of free energy changes, ΔG, for reactions involving SQ in the Q_o site require accurate one- and two-electron redox potentials and pK_a values for all the $Q/SQ/QH_2$ species bound to the protein at Q_o. Measurement of many of the required quantities has not been experimentally possible. However, for the series of closely-related *p*-benzoquinone derivatives used here, the redox potentials and pK_a values in the Q_o site should be offset from the corresponding aqueous solution values by a similar amount if there are no strong specific interactions affecting some molecules in the series much more than the others. The ΔG for a reaction in the protein should be shifted by a similar amount. Thus, the change in free energy

of reaction, ΔΔG, for different substrate analogs in this series should be similar whether estimated using the inaccessible values in the protein or the values in aqueous solution.

The use of aqueous properties has its own challenges. Aqueous redox potentials from cyclic voltammetric measurements are not reliable for many lipophilic quinone species (43,52,53). Moreover, the reduction potential for Q to $Q^{\bullet -}$ (or the oxidation of QH_2 to $QH^{\bullet}$ or $Q^{\bullet -}$) is nearly impossible to measure reliably by experiment in aqueous solution due to the disproportionation of the semiquinone species in the solutions. Fortunately, there is sufficient experimental data to support the calculation of aqueous redox potentials and pK_as in this series of substrate analogs. We use procedures which predict reasonably accurate aqueous redox potentials across a series of homologous water-soluble quinone species (43), similar to 'benchmarking' approaches used successfully in other cases to predict accurate redox potentials and pK_a values (54,55). The computed values are summarized in Table 2 with full details in the Supporting Information.

Results

Kinetics of Superoxide Production in AA-inhibited Complexes

The apparent Michaelis constant (K_m) and the maximum velocity of superoxide production (V_{max}) were determined for substrates (1)-(7), Scheme 1 and Table 1. The K_m values reflect the partition coefficient for each substrate analog into the detergent or membrane and the apparent binding constant at the Q_o site. The K_m for all substrate analogs lie in the range of 5–35 μM except for (4), which has solubility problems and a large apparent K_m ~150 μM.

For several substrates, the AA-inhibited turnover assays slowed markedly as the product Q accumulated. Such behavior has been observed for other non-native substrates (19,45) and indicates product inhibition, that is, the oxidized substrate binds more tightly to Q_o than the substrate itself. Product inhibition implies that the Q/QH_2 redox potential shifts to more negative values when bound at Q_o. To measure those shifts, binding constants for the oxidized substrates at Q_o were estimated from competition assays on uninhibited, steady-state turnover driven by decyl-ubiquinol. The data was analyzed with mixed competition kinetics with competitive inhibition considered to be binding of the quinol at the Q_o site and the non-competitive inhibition as binding of the Q at a site distinct from the Q_o binding pocket, probably the Q_i site. The K_i values were significant only for four substrates and the calculated shift in the redox potential $E_m(Q/QH_2)$ based on the K_m and competitive K_i values range from −0.003 to −0.060 V, less than the uncertainty in calculated redox potential and much less than the range of potentials for (1)-(7).

Superoxide Production Rates Are Related to the Potentials for SQ Formation

The V_{max} for superoxide production varies by more than two orders of magnitude for substrates (1)-(7) and depends strongly on the relative redox potential for the one-electron oxidation of (1)-(7), Figure 2. Remarkably, the present data plotted as a function of the shift in oxidation potential of QH_2 relative to UQH_2 forms a smooth extension of the Forquer, *et al.* (34) data plotted as a function of the reduction potential shifts of the Rieske ISP (as varied by site-directed mutagenesis in *S. cerevisiae*). The reaction rate varies consistently with changes in the redox potential of the QH_2/ISP couple whether the redox potential of the substrate or of the ISP is changed. This combined data shows that the rate limiting step for superoxide generation depends on the redox potential for the one-electron reduction of the Rieske ISP by substrate.

The relation is equally strong whether we consider the redox potential for the $QH^{\bullet}/QH_2$ or $Q^{\bullet -}/QH_2$ couples, Figure 2. The semiquinones of (**1**)-(7) all have similar pK_a values, Table 1, which forces the potentials for oxidation of QH_2 to $QH^{\bullet}$ or $Q^{\bullet -}$ to shift by similar amounts.

Notably, there is no correlation between the rate of superoxide production and the potential for the second electron transfer, Figure 3, indicating that the oxidation of SQ_o is not rate limiting for the production of superoxide.

Discussion

Specific Molecular Interactions Do Not Have Large Effects on Superoxide Production

Alterations to the QH_2 substrate of the Q_o site can cause the cyt bc_1 complex to produce superoxide at rates exceeding that of normal Q-cycle turnover (~100 s^{-1}), Figure 2 and previous work (19). Altering the substrate could elicit rapid superoxide production by altering specific interactions between the binding site and the substrate that are crucial for steering or gating the reaction into products; or by changing the driving force for formation or subsequent reaction of SQ_o. The current work was designed to distinguish between these possibilities by probing superoxide production with a homologous series of synthetic substrate analogs.

The substrate analogs were selected, in part, to vary the sidegroups on the benzoquinone ring available to participate in specific interactions with the Q_o site. Aside from the obvious effects of ring substituents on redox potentials (see below), there is no discernable relation between superoxide production and the position or type of ring substituent in (1)-(7). The quinol –OH groups and the hydrocarbon tail are certainly necessary for activity; yet, groups at other positions can change the V_{max} by two orders of magnitude! The V_{max} for superoxide production in AA-inhibited complex is little affected by which hydrophobic tail is attached, with undecylubiquinol, (3), decylubiquinol (34), and ubiquinol-3 (19) giving essentially equal rates. The position and the identity of individual chloro-, methyl-, methoxy-, or amino- sidegroups also are not decisive in determining the V_{max} for superoxide production (except through their overall influence on the redox potential, see below). The rate of electron transfer from a substrate analog in this series bound at the Q_o site is not controlled by the physical structure of the substrate analog.

Superoxide Production Rates are Controlled by the Driving Force for SQ_o Formation

The substrate analogs were also selected to provide large variations in both Q/QH_2 redox potential and semiquinone stability constant, K_s, Table 2. The large scatter in K_s means that the potential or driving force for the first electron transfer does not track the potential for the second electron transfer (from SQ_o to O_2) and makes it possible to distinguish between the first and second electron transfer reactions. The V_{max} for superoxide production increases as the quinol becomes a better one-electron reducing agent and as the Rieske ISP becomes easier to reduce (34), Figure 2. That is, the rate of the reaction depends on the driving force for the one-electron oxidation of the substrate by the Rieske ISP but not on the driving force for the oxidation of SQ_o. Thus, the rate limiting step with saturating substrate concentrations in superoxide production is the direct, one-electron oxidation of QH_2 by the ISP to produce SQ_o and reduced ISP. Because the activation energy with the natural substrate (34) for this step is the same as for the normal Q-cycle, the first electron transfer step in the bifurcated oxidation of quinol in the cyt bc_1 complex must also be the direct, one-electron oxidation of QH_2 by the ISP. Covian and Trumpower (42) recently reported that the first electron transfer step is no longer the rate limiting step at less than saturating substrate concentrations. They concluded that the rate limitation occurs at a different step for normal turnover than for the bypass reactions that occur under their conditions. That report did not determine where the rate limitation moved in the complicated, multi-step reactions pathway of the cyt bc_1 complex, or whether the bypass reactions under those new conditions results in superoxide production.

Superoxide is Produced by SQ

Figures 2 and 3 clearly show that the rate limiting step for superoxide production is the first electron transfer. But what is the immediate source of the electron to convert O_2 into superoxide--the reduced Rieske ISP; the reduced cyt b_L; or SQ_o? It is not likely the Rieske ISP. In contrast to the FeS cluster in Complex I, the reduced Rieske ISP is rather stable in air-saturated solutions either as part of the cyt bc_1 complex or as the purified protein owing to its unusually high redox potential (~+0.275 V at pH = 7.0) (56). Its ability to reduce oxygen is incapable of supporting the measured superoxide production rates. Furthermore, measurements of bypass reactions in the cyt bc_1 complex find that at least one electron per quinol makes it through the high-potential chain (21, 22), safely passing through the Rieske ISP. An electron that enters the high-potential chain at the Rieske ISP apparently is not easily diverted to superoxide.

The electron to convert O_2 to superoxide therefore must come from SQ_o but its path to O_2 is not obvious. Electron transfer from SQ_o through heme b_L or the low-potential chain to produce superoxide is one possibility. The proximal niche inhibitors myxothiazol or MOA stilbene (21,22) prevent electrons from entering the low-potential chain, yet elicit substantial amounts of such superoxide from the cyt bc_1 complex. Muller, *et al*. (21) showed that V_{max} for superoxide production in the presence of proximal niche inhibitors is roughly half that of AA-inhibited complexes. This provides a clear demonstration that reduced cyt b_L is not an essential precursor to superoxide because proximal niche inhibitors prevent electrons from entering the low-potential chain and reducing cyt b_L. Moreover, when electrons can enter the low-potential chain, as with AA inhibition, the steady state accumulation of electrons on cyt b_L ought to cause superoxide production at rates proportional to the amount of reduced cyt b_L. Presently available data do not support this prediction (19); very reducing substrates such as rhodoquinol generate similar steady state levels of reduced cyt *b* as ubiquinol even though superoxide production rates differ by ~2 orders of magnitude. Thus, the low-potential chain does not appear to be able to pass electrons efficiently from SQ_o to superoxide.

SQ_o is the only remaining plausible source of the electron for superoxide production and SQ_o must therefore be considered the last known predecessor of superoxide. However, there is little direct data to indicate whether SQ_o reacts in the Q_o site to produce superoxide or after escape from the Q_o site.

Recent studies of superoxide production during ‘semi-reverse’ electron flow (32,33) conclude that under extreme conditions, electron flow in the low-potential chain can be reversed, with electrons flowing from the Q_i site to the Q_o site, to reduce quinone in the Q_o site to SQ_o and then producing superoxide. That route to superoxide production supports our results that SQ_o is the last known precursor to superoxide.

Superoxide Production Shares Intermediates with the Q-Cycle

Superoxide production rates at saturating substrate concentrations are related to shifts in redox potential of both the Rieske ISP and the quinol substrate, Figure 2. The relationship can be summarized following Crofts, *et al.*, p. 1023 (23), based on Marcus Theory as:

$$v \propto \mathrm{Exp}\left[-\frac{\Delta\Delta G}{RT}\right] \propto \mathrm{Exp}\left[-F\frac{E(SQ/QH_2) - E(ISP_{ox}/ISP_{red})}{RT}\right]$$

This equation has been experimentally tested by variation of the ISP redox potential for normal Q-cycle turnover (23,34) and for superoxide production (23). We now find that it holds when the redox potential of the substrate is varied. Thus, the free energy change for the one-electron

transfer from substrate to the ISP predicts the rate of superoxide production. This indicates that the rate-limiting step for superoxide production is the one-electron transfer reaction to produce SQ_o (either as the neutral radical or as the radical anion) and reduced ISP. The activation energies at saturating substrate concentrations are the same for superoxide production and for oxidation of quinol in the Q-cycle (34), indicating the same rate limiting step in both processes. The paths then diverge at SQ_o or soon thereafter as proposed earlier (23,34).

The initial electron transfer is thought to occur in a hydrogen-bonded complex between quinol and a histidine ligand of the FeS cluster (23,32,34,57). In such a 'contact ion pair', back electron transfer should be rapid. A distinct SQ_o would appear only after the contact ion pair moves apart and back electron transfer slows dramatically, to kinetically 'trap' SQ_o so that it reacts with O_2 or proceeds along the Q-cycle. The motion of the ISP headgroup to carry its FeS cluster to cyt c_1 is the obvious way for the contact ion pair to dissociate and to terminate the electron transfer step. This view predicts that blocking movement of the ISP would prevent formation of SQ_o and superoxide. Indeed, Borek, *et al.* (32) reported no superoxide production in the double alanine insertion mutant of the ISP, where ISP movement is blocked (56). This observation was explained by a gating mechanism in which "the structural changes that occur in the Q_o site upon movement of FeS" "act to transiently 'open' the Q_o site for the reaction with oxygen" (32). The 'opening' of this gate is perhaps best viewed in a general sense in which a fully reactive SQ_o is not formed until the ISP has moved away from Q_o.

Conclusion

Mounting evidence shows that some of the bypass reactions, particularly those producing superoxide during oxidation of quinol at the Q_o site, diverge from the Q-cycle rather late in the bifurcated reaction. Consequently bypass reactions provide an additional means of studying the initial reactions of the Q-cycle as demonstrated here. There is more scope for controlling and manipulating reaction conditions, *e.g.*, varying redox potential, because the bypass reactions effectively isolate or decouple the initial reactions in the Q-cycle from later steps, avoiding many complications and interactions. We used that approach here to examine the dependence of oxidation rate on the redox potential and structure of the substrate. We find that the direct one-electron oxidation of QH_2 by the Rieske ISP produces a semiquinone during oxidation of quinol at the Q_o site in the Q-cycle and in superoxide production. The oxidation of the semiquinone and the reduction of cyt *b* or O_2 are subsequent steps, distinct from the rate limiting step. The production of superoxide whether through the oxidation of quinol in the Q_o site studied here or through the reduction of quinone in the Q_o site by reversed electron flow (32,33) involves the generation of SQ_o which is the last known precursor to superoxide. At lower substrate concentrations, other reactions become rate limiting and detailed measurements of carefully designed mutants and substrate analogs or of kinetic isotope effects can make substantial contributions to determining the entire reaction network.

These experimental results reported here are incompatible: 1) with models for cyt bc_1 in which electron transfer to the high-potential chain is not a distinct step preceding electron transfer to the low-potential chain, and 2) with conformational gating models that would produce superoxide by a very different set of reactions from the normal Q-cycle.

Supplementary Material

Refer to Web version on PubMed Central for supplementary material.

Acknowledgments

The authors acknowledge many useful discussions, in particular with Wolfgang Nitschke, Fevzi Daldal, Christopher Moser, P. Leslie Dutton, Antony R. Crofts, and Isaac Forquer. The authors also thank Daniel Vasseo and Michael Jourdes for their technical assistance.

References

1. Crofts AR. The cytochrome bc_1 complex: Function in the context of structure. Annual Review of Physiology 2004;66:689–733.
2. Berry EA, Guergova-Kuras M, Huang LS, Crofts AR. Structure and function of cytochrome *bc* complexes. Annu Rev Biochem 2000;69:1005–1075. [PubMed: 10966481]
3. Schutz M, Brugna M, Lebrun E, Baymann F, Huber R, Stetter KO, Hauska G, Toci R, Lemesle-Meunier D, Tron P, Schmidt C, Nitschke W. Early evolution of cytochrome *bc* complexes. J Mol Biol 2000;300:663–675. [PubMed: 10891261]
4. Nitschke, W.; Kramer, DM.; Riedel, A.; Liebl, U. From naphtho-to benzoquinones — (R)evolutionary reorganizations of electron transfer chains. In: Mathis, P., editor. Photosynthesis: From Light to Biosphere. Kluwer Academic Publishers; Dordrecht: 1995. p. 945-948.
5. Iwata S, Lee JW, Okada K, Lee JK, Iwata M, Rasmussen B, Link TA, Ramaswamy S, Jap BK. Complete structure of the 11-subunit bovine mitochondrial cytochrome bc_1 complex. Science 1998;281:64–71. [PubMed: 9651245]
6. Crofts, AR.; Berry, EA.; Kuras, R.; Guergova-Kuras, M.; Hong, S.; Ugulava, NB. Structures of the bc_1 complex reveal dynamic aspects of mechanism. In: Garab, G., editor. Photosynthesis: Mechanisms and Effects. Kluwer Academic Publ; Dordrecht: 1999. p. 1481-1486.
7. Hunte C, Palsdottir H, Trumpower BL. Protonmotive pathways and mechanisms in the cytochrome bc_1 complex. FEBS Letters 2003;545:39–46. [PubMed: 12788490]
8. Esser L, Quinn B, Li YF, Zhang MQ, Elberry M, Yu L, Yu CA, Xia D. Crystallographic Studies of Quinol Oxidation Site Inhibitors: a Modified Classification of Inhibitors for the Cytochrome bc_1 Complex. Journal of Molecular Biology 2004;341:281–302. [PubMed: 15312779]
9. Mitchell P. The protonmotive Q cycle: A general formulation. FEBS Letters 1975;59:137–139. [PubMed: 1227927]
10. Crofts AR, Shinkarev VP, Kolling DRJ, Hong SJ. The Modified Q-Cycle Explains the Apparent Mismatch Between the Kinetics of Reduction of Cytochromes c_1 and b_H in the bc_1 Complex. Journal of Biological Chemistry 2003;278:36191–36201. [PubMed: 12829696]
11. Crofts AR, Wang Z. How rapid are the internal reactions of the ubiquinol: cytochrome c_2 oxidoreductase? Photosynthesis Research 1989;22:69–87.
12. Crofts AR, Wraight CA. The Electrochemical Domain of Photosynthesis. Biochim Biophys Acta 1983;726:149–185.
13. Berry EA, Huang LS. Observations Concerning the Quinol Oxidation Site of the Cytochrome bc_1 Complex. Febs Letters 2003;555:13–20. [PubMed: 14630312]
14. Cape JL, Bowman MK, Kramer DM. A semiquinone intermediate generated at the Q_o site of the cytochrome bc_1, complex: Importance for the Q-cycle and superoxide production. Proceedings of the National Academy of Sciences of the United States of America 2007;104:7887–7892. [PubMed: 17470780]
15. Zhang HB, Osyczka A, Dutton PL, Moser CC. Exposing the complex III Q_o semiquinone radical. Biochimica Et Biophysica Acta-Bioenergetics 2007;1767:883–887.
16. Schultz BE, Chan SI. Structures and proton-pumping strategies of mitochondrial respiratory enzymes. Annual Review of Biophysics and Biomolecular Structure 2001;30:23–65.
17. Wenz T, Hellwig P, MacMillan F, Meunier B, Hunte C. Probing the role of E272 in quinol oxidation of mitochondrial complex III. Biochemistry 2006;45:9042–9052. [PubMed: 16866349]
18. Cape JL, Bowman MK, Kramer DM. Understanding the Cytochrome *bc* Complexes by What They Don't Do. The Q-Cycle at 30. Trends in Plant Science 2006;11:46–55. [PubMed: 16352458]
19. Cape JL, Strahan JR, Lenaeus MJ, Yuknis BA, Trieu TL, Shepherd JN, Bowman MK, Kramer DM. The Respiratory Substrate Rhodoquinol Induces Q-cycle Bypass Reactions in the Yeast Cytochrome

bc$_1$ Complex: Mechanistic and Physiological Implications. Journal of Biological Chemistry 2005;280:34654–34660. [PubMed: 16087663]

20. Kramer DM, Roberts AG, Muller FL, Cape J, Bowman MK. Q-cycle Bypass Reactions at the Q_o site of the Cytochrome *bc*$_1$ (and Related) Complexes. Methods in Enzymology 2004;382:21–45. [PubMed: 15047094]
21. Muller FL, Roberts AG, Bowman MK, Kramer DM. Architecture of the Q_o site of the cytochrome *bc*$_1$ complex probed by superoxide production. Biochemistry 2003;42:6493–6499. [PubMed: 12767232]
22. Muller F, Crofts AR, Kramer DM. Multiple Q-cycle bypass reactions at the Q_o site of the cytochrome *bc*$_1$ complex. Biochemistry 2002;41:7866–7874. [PubMed: 12069575]
23. Crofts AR, Lhee S, Crofts SB, Cheng J, Rose S. Proton pumping in the *bc*$_1$ complex: A new gating mechanism that prevents short circuits. Biochimica Et Biophysica Acta-Bioenergetics 2006;1757:1019–1034.
24. Mulkidjanian AY. Ubiquinol oxidation in the cytochrome *bc*$_1$ complex: Reaction mechanism and prevention of short-circuiting. Biochimica Et Biophysica Acta-Bioenergetics 2005;1709:5–34.
25. Osyczka A, Moser CC, Dutton PL. Fixing the Q cycle. Trends in Biochemical Sciences 2005;30:176–182. [PubMed: 15817393]
26. Rich PR. The quinone chemistry of BC complexes. Biochim Biophys Acta-Bioenergetics 2004;1658 (Supplement S):32–32.
27. Osyczka A, Moser CC, Daldal F, Dutton PL. Reversible Redox Energy Coupling in Electron Transfer Chains. Nature 2004;427:607–612. [PubMed: 14961113]
28. Shinkarev VP, Crofts AR, Wraight CA. The electric field generated by photosynthetic reaction center induces rapid reversed electron transfer in the *bc*$_1$ complex. Biochemistry 2001;40:12584–12590. [PubMed: 11601982]
29. Tahara EB, Navarete FDT, Kowaltowski AJ. Tissue-, substrate-, and site-specific characteristics of mitochondrial reactive oxygen species generation. Free Radical Biology and Medicine 2009;46:1283–1297. [PubMed: 19245829]
30. Rottenberg H, Covian R, Trumpower BL. Membrane potential greatly enhances superoxide generation by the cytochrome *bc*$_1$ complex reconstituted into phospholipid vesicles. J Biol Chem 2009:M109.017376.
31. Fisher N, Castleden CK, Bourges I, Brasseur G, Dujardin G, Meunier B. Human Disease-Related Mutations in Cytochrome *b* Studied in Yeast. Journal of Biological Chemistry 2004;279:12951–12958. [PubMed: 14718526]
32. Borek A, Sarewicz M, Osyczka A. Movement of the Iron-Sulfur Head Domain of Cytochrome *bc*$_1$ Transiently Opens the Catalytic Q_o Site for Reaction with Oxygen. Biochemistry 2008;47:12365–12370. [PubMed: 18956890]
33. Drose S, Brandt U. The Mechanism of Mitochondrial Superoxide Production by the Cytochrome *bc*$_1$ Complex. J Biol Chem 2008;283:21649–21654. [PubMed: 18522938]
34. Forquer I, Covian R, Bowman MK, Trumpower BL, Kramer DM. Similar transition states mediate the Q-cycle and superoxide production by the cytochrome *bc*$_1$ complex. Journal of Biological Chemistry 2006;281:38459–38465. [PubMed: 17008316]
35. Hong SJ, Ugulava N, Guergova-Kuras M, Crofts AR. The Energy Landscape for Ubihydroquinone Oxidation at the Q_o Site of the *bc*$_1$ Complex in *Rhodobacter Sphaeroides*. Journal of Biological Chemistry 1999;274:33931–33944. [PubMed: 10567355]
36. Trumpower BL. A Concerted, Alternating Sites Mechanism of Ubiquinol Oxidation by the Dimeric Cytochrome *bc*$_1$ Complex. Biochimica Et Biophysica Acta-Bioenergetics 2002;1555:166–173.
37. Lange C, Hunte C. Crystal structure of the yeast cytochrome *bc*$_1$ complex with its bound substrate cytochrome *c*. Proceedings of the National Academy of Sciences of the United States of America 2002;99:2800–2805. [PubMed: 11880631]
38. Darrouzet E, Valkova-Valchanova M, Moser CC, Dutton PL, Daldal F. Uncovering the [2Fe2S] Domain Movement in Cytochrome *bc*$_1$ and its Implications for Energy Conversion. Proceedings of the National Academy of Sciences of the United States of America 2000;97:4567–4572. [PubMed: 10781061]

39. Darrouzet E, Valkova-Valchanova M, Ohnishi T, Daldal F. Structure and function of the bacterial bc_1 complex: Domain movement, subunit interactions, and emerging rationale engineering attempts. Journal of Bioenergetics and Biomembranes 1999;31:275–288. [PubMed: 10591533]
40. Crofts, AR. The bc_1 Complex: What is There Left to Argue About?. In: Wikstrom, M., editor. Biophysical and Structural Aspects of Bioenergetics. Royal Society of Chemistry; Cambridge: 2006. p. 123-155.
41. Iwata M, Bjorkman J, Iwata S. Conformational change of the Rieske [2Fe-2S] protein in cytochrome bc_1 complex. J Bioenerg Biomembr 1999;31:169–175. [PubMed: 10591523]
42. Covian R, Trumpower BL. The Rate-limiting Step in the Cytochrome bc_1 Complex (Ubiquinol-Cytochrome c Oxidoreductase) Is Not Changed by Inhibition of Cytochrome *b*-dependent Deprotonation: Implications for the Mechanism of ubiquinol Oxidation at Center P of the bc_1 Complex. J Biol Chem 2009;284:14359–14367. [PubMed: 19325183]
43. Cape JL, Bowman MK, Kramer DM. Computation of the redox and protonation properties of quinones: Towards the prediction of redox cycling natural products. Phytochemistry 2006;67:1781–1788. [PubMed: 16872647]
44. Folkers K, Catlin JC, Daves GD. Coenzyme Q. 124. New substituted 2,3-dimethoxy-1,4-benzoquinones as inhibitors of coenzyme Q systems. Journal of Medicinal Chemistry 1971;14:45–48. [PubMed: 5539745]
45. Gu LQ, Yu L, Yu CA. Effect Of Substituents Of The Benzoquinone Ring On Electron-Transfer Activities Of Ubiquinone Derivatives. Biochimica Et Biophysica Acta 1990;1015:482–492. [PubMed: 2154255]
46. Keegstra EMD, Huisman BH, Paardekooper EM, Hoogesteger FJ, Zwikker JW, Jenneskens LW, Kooijman H, Schouten A, Veldman N, Spek AL. 2,3,5,6-tetraalkoxy-1,4-benzoquinones and structurally related tetraalkoxy benzene derivatives: Synthesis, properties and solid state packing motifs. Journal of the Chemical Society-Perkin Transactions 1996;2:229–240.
47. Gu LQ, Yu L, Yu CA. A ubiquinone derivative that inhibits mitochondrial cytochrome bc_1 complex but not chloroplast cytochrome b_6f complex activity. J Biol Chem 1989;264:4506–4512. [PubMed: 2538447]
48. Ljungdahl PO, Pennoyer JD, Robertson DE, Trumpower BL. Purification of highly active cytochrome bc_1 complexes from phylogenetically diverse species by a single chromatographic procedure. Biochimica et Biophysica Acta (BBA) -Bioenergetics 1987;891:227–241.
49. Fisher N, Bourges I, Hill P, Brasseur G, Meunier B. Disruption of the interaction between the Rieske iron-sulfur protein and cytochrome *b* in the yeast bc_1 complex owing to a human disease-associated mutation within cytochrome *b*. European Journal of Biochemistry 2004;271:1292–1298. [PubMed: 15030479]
50. Wenz T, Covian R, Hellwig P, MacMillan F, Meunier B, Trumpower BL, Hunte C. Mutational analysis of cytochrome *b* at the ubiquinol oxidation site of yeast complex III. Journal of Biological Chemistry 2007;282:3977–3988. [PubMed: 17145759]
51. Fresht, A. Enzyme Structure and Mechanism. W. H. Freeman; San Francisco: 1977 .
52. Marchal D, Boireau W, Laval JM, Moiroux J, Bourdillon C. An electrochemical approach of the redox behavior of water insoluble ubiquinones or plastoquinones incorporated in supported phospholipid layers. Biophysical Journal 1997;72:2679–2687. [PubMed: 9168043]
53. Michalkiewicz S. Cathodic reduction of coenzyme Q_{10} on glassy carbon electrode in acetic acid-acetonitrile solutions. Bioelectrochemistry 2007;70:495–500. [PubMed: 17046336]
54. Baik MH, Friesner RA. Computing redox potentials in solution: Density functional theory as a tool for rational design of redox agents. Journal of Physical Chemistry A 2002;106:7407–7412.
55. Fu Y, Liu L, Wang YM, Li JN, Yu TQ, Guo QX. Quantum-chemical predictions of redox potentials of organic anions in dimethyl sulfoxide and reevaluation of bond dissociation enthalpies measured by the electrochemical methods. Journal of Physical Chemistry A 2006;110:5874–5886.
56. Cooley JW, Roberts AG, Bowman MK, Kramer DM, Daldal F. The Raised Midpoint Potential of the [2Fe2S] Cluster of Cytochrome bc_1 Is Mediated by Both the Q_o Site Occupants and the Head Domain Position of the Fe-S Protein Subunit. Biochemistry 2004;43:2217–2227. [PubMed: 14979718]

57. Cape JL, Bowman MK, Kramer DM. Reaction Intermediates of Quinol Oxidation in a Photoactivatable System That Mimics Electron Transfer in the Cytochrome bc_1 Complex. Journal of the American Chemical Society 2005;127:4208–4215. [PubMed: 15783202]

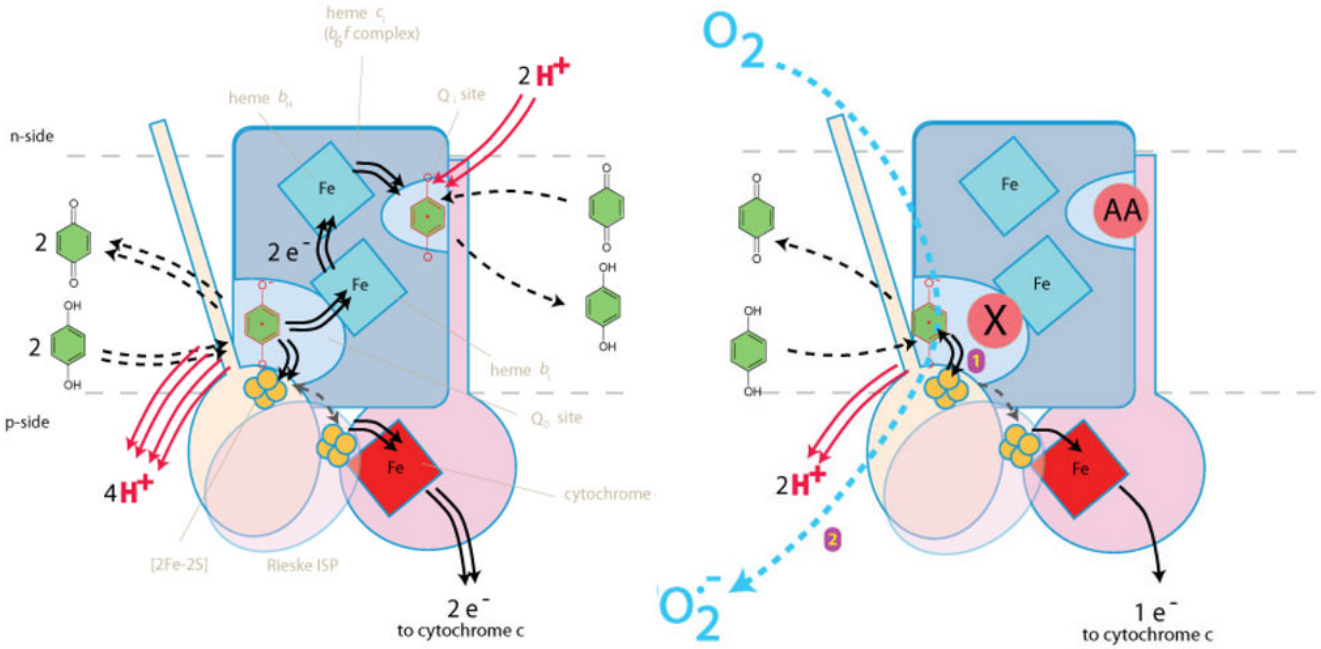

Figure 1. The uninhibited Q-cycle and superoxide production under partially inhibited conditions

Left) The Q-cycle, showing how two turnovers at the Q_o site sends two electrons through the high-potential chain to cyt *c*, and two electrons through the low-potential chain to reduce a quinone bound at the Q_i site. These reactions release four protons from QH_2 at the Q_o site (red arrows), and the take up two protons by Q at the Q_i site (red arrows), resulting in a net $2H^+/e^-$ translocation stoichiometry. **Right**) Blockage of the low-potential chain prevents transfer of the second QH_2 electron following the initial transfer to the high-potential chain. The reactive SQ intermediate accumulates in Q_o and can reduce oxygen to form superoxide (blue arrow), or participate in other non-productive 'bypass reactions'. Both panels show pivoting of the Rieske ISP, which partially gates reactions of the SQ to prevent double reduction of the high-potential chain.

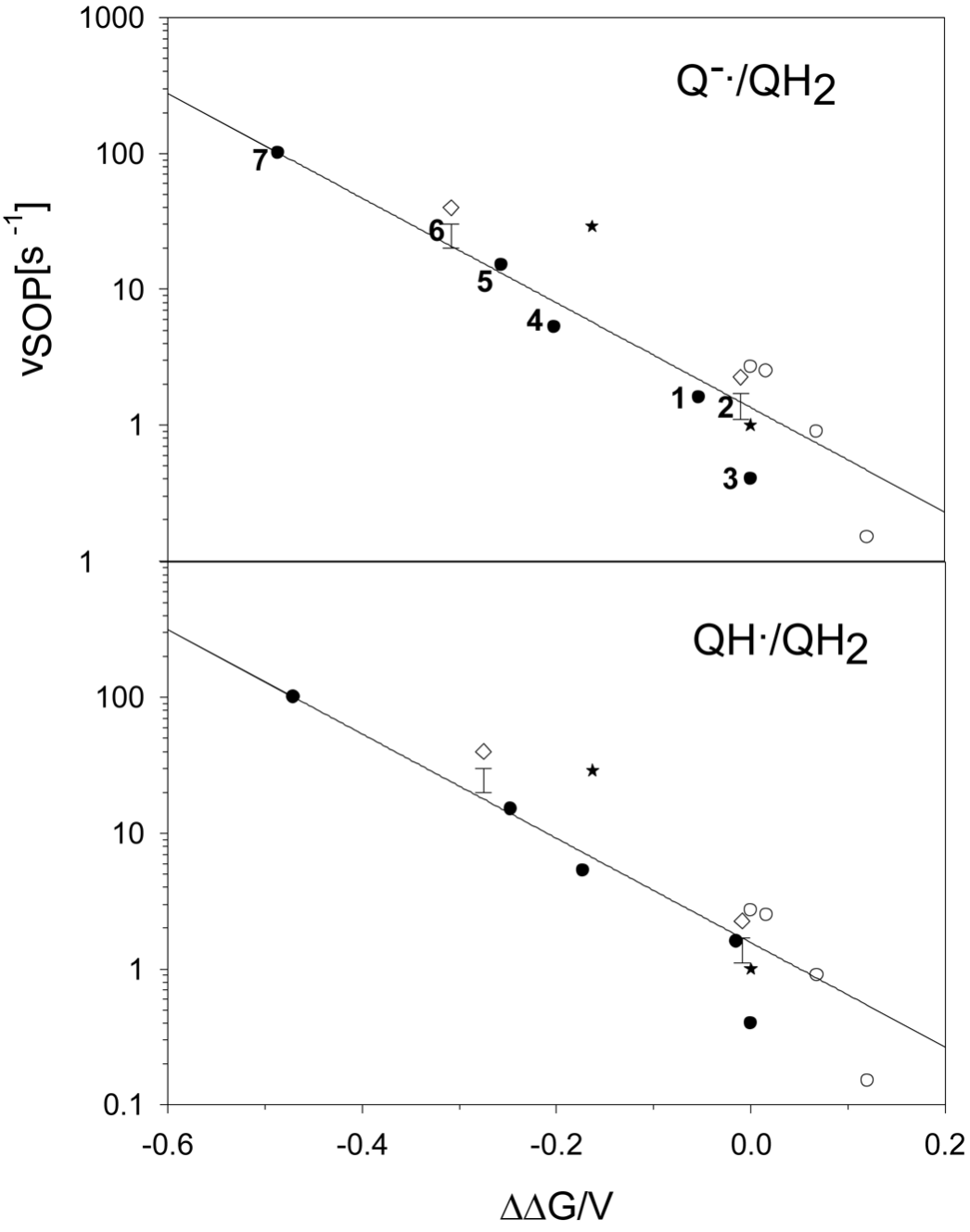

Figure 2.

The V_{max} for superoxide production, v_{SOP}, in μmoles of superoxide per μmole of cyt bc_1 s^{-1} measured with saturating amounts of substrate analog and corresponding to V_{max}. Rates are plotted as a function of the shift, ΔΔG, in oxidation potential for substrate analogs (**Upper** for $QH_2/Q^{-\bullet}$; **Lower** for $QH_2/QH^{\bullet}$) or reduction potential for the Rieske ISP. (●) v_{SOP} for substrate analogs from Table 1, the analog is indicated by number to the left of the symbol; (○) v_{SOP} for Rieske ISP mutants from Forquer, *et al.*(34) measured using the Amplex Red assay; (*) v_{SOP} for substrate analogs UQ_3 and RQ_3 from Cape, *et al.*(19); (◇) V_{max} for total bypass in μmoles

of substrate analog oxidized per μmole of cyt bc_1 s^{-1} for (2) and (6) with the typical range for the v_{SOP} indicated directly below by ‘error’ bars.

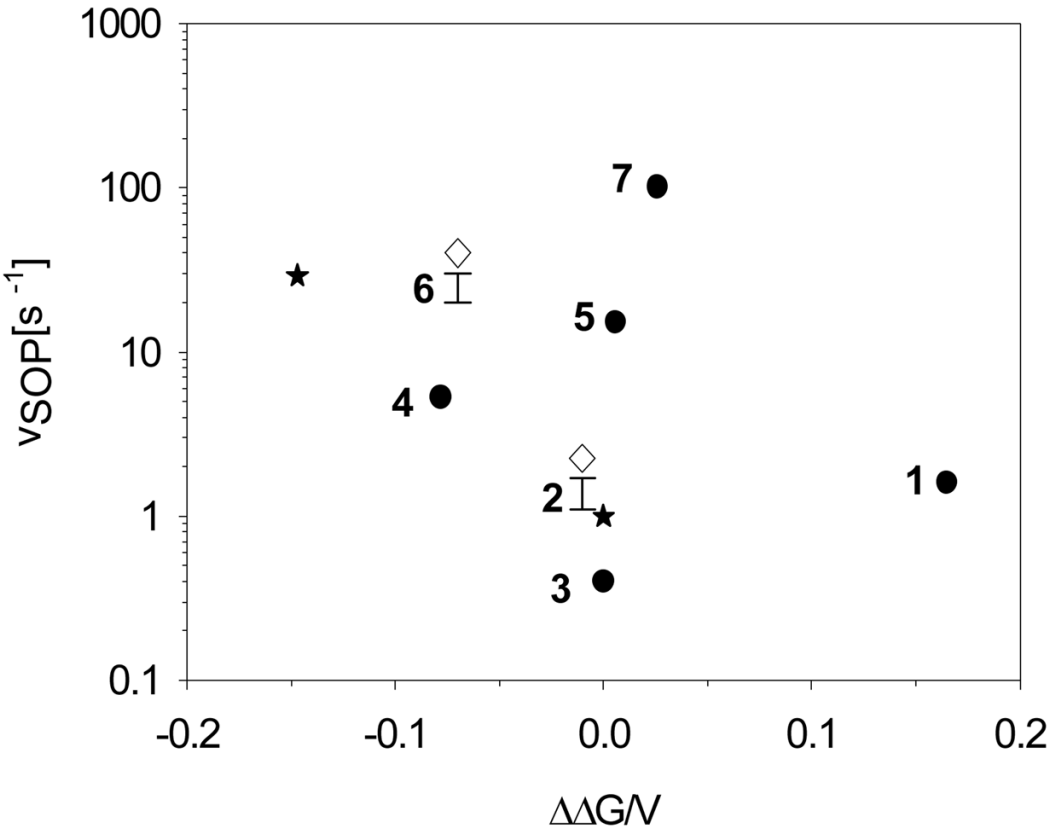

Figure 3.
The V_{max} for superoxide production, v_{SOP}, in μmoles of superoxide per μmole of cyt bc_1 s^{-1} measured with saturating amounts of substrate analog. Rates are plotted as a function of the shift in oxidation potential for substrate analogs for QH_2/Q. Symbols are the same as in Figure 2A.

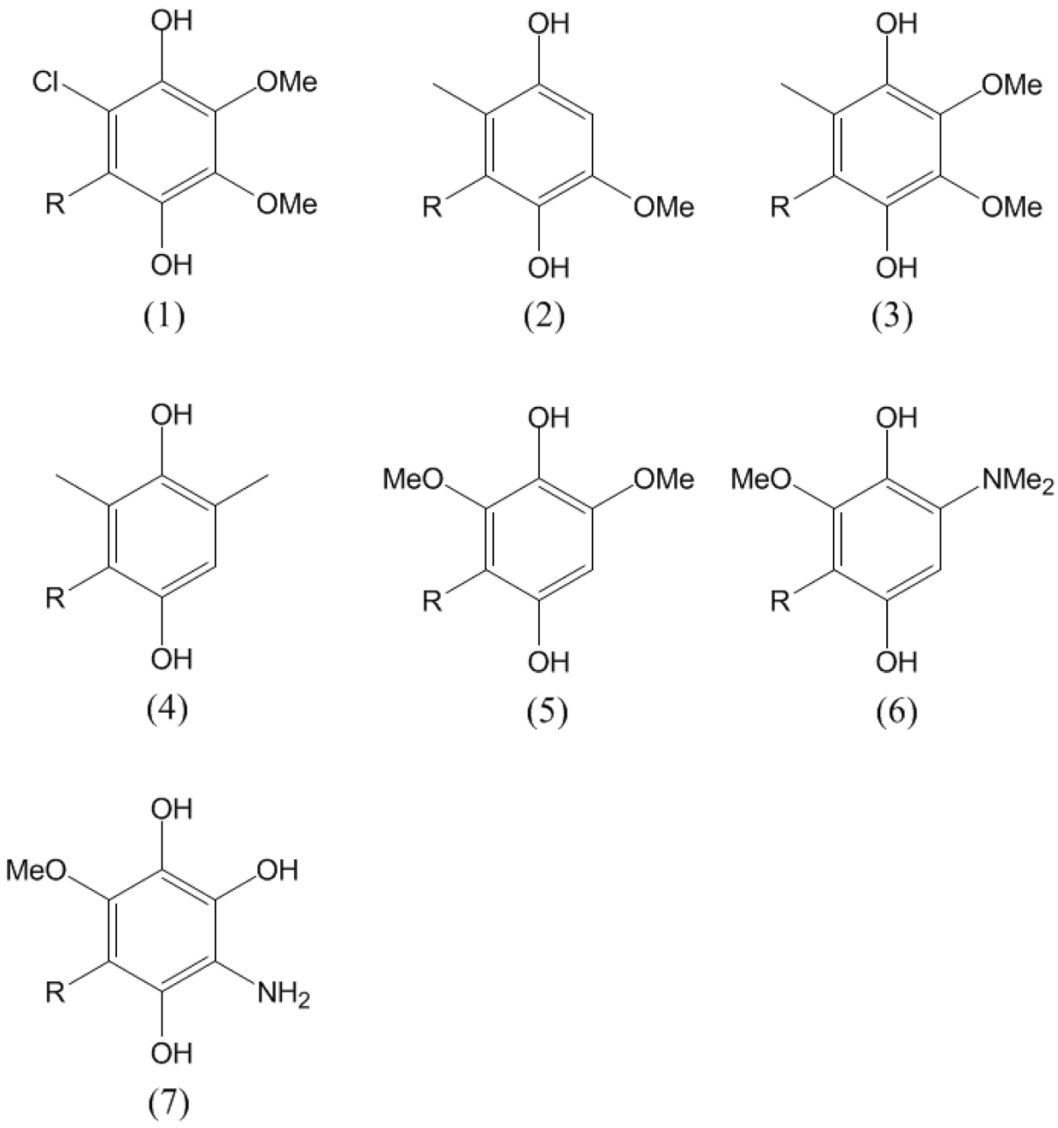

Scheme 1.
Synthetic QH_2 substrates. -R denotes the *n*-undecyl group, $-C_{11}H_{23}$.

Table 1

Kinetic parameters for steady state turnover of AA-inhibited cyt bc_1 complex. f_{SOP} is the fraction of Q-cycle bypass reactions resulting in superoxide production derived from the superoxide dismutase sensitivity of cyt *c* reduction in the AA-inhibited complex. Product inhibition constants K_i for a mixed inhibition model are for uninhibited steady –state turnover driven by decyl-ubiquinol. K_m and K_i are reported in units of μM. Rates of quinol oxidation are given in s^{-1} from total bypass reactions (V_{max}(bypass)) and from superoxide-producing bypass reaction (V_{max}(SO)). In two cases, V_{max}(SO) could not be measured but is estimated as a range: 0.5–0.75 V_{max}(bypass) covering the range of measured f_{SOP}. Rates noted in italics were measured by stopped flow. The shift in redox potential for the Q/QH_2 couple based on measured values of K_m and the competitive K_i are reported in V.

Substrate	K_m	V_{max}**(bypass)**	f_{SOP}	V_{max}**(SO)**	K_i**(C)**	K_i **(NC)**	ΔE_m
(1)	23	2.4	0.68	1.6	2.1	-	−0.060
(2)	25	2.2	-	1.1–1.7	11.8	5.8	−0.019
(3)	5	0.6	0.66	0.4	-	-	-
(4)	>150	7.5	0.71	5.3	-	-	-
(5)	9	27	0.55	15.1	4.4	7.1	−0.018
(6)	35	*80*	-	*40–60*	-	-	-
(7)	30	*199*	0.51	*101*	26.2	36.8	−0.003

Table 2

Calculated aqueous redox potentials and pK_a values for SQ species, estimated K_s values, and SQ/QH_2 potentials for protonated and deprotonated SQ species. K_S is defined as the the equilibrium constant for comproportionation of $Q + QH_2$ to form 2 $QH^{\bullet}$. All potentials and equilibrium constants are adjusted to the experimental conditions of pH 8.0. Redox potentials are given in V versus the standard hydrogen electrode.

Substrate	$E(Q/QH_2)$	$E(Q/Q^{\bullet-})$	$pK_{a\ SQ}$	log K_S	$E(QH^{\bullet}/QH_2)$	$E(Q^{\bullet-}/QH_2)$
(1)	0.178	0.087	4.70	−9.66	0.463	0.269
(2)	0.112	−0.088	5.33	−12.09	0.469	0.312
(3)	0.122	−0.078	5.35	−12.05	0.478	0.322
(4)	−0.018	−0.156	4.86	−10.93	0.305	0.12
(5)	−0.003	−0.072	5.19	−7.94	0.231	0.066
(6)	−0.067	−0.148	4.79	−9.14	0.203	0.014
(7)	−0.108	−0.052	5.10	−3.89	0.007	−0.164